Supporting Information

Multiepitope glycan based laser assisted fluorescent nanocomposite with dual functionality for sensing and ablation of *Pseudomonas aeruginosa*

Priyanka Garg[ab#], Nitesh Priyadarshi[ab#], Mayur D. Ambule[cd#], Gurmeet Kaur[e], Sunaina Kaul[ab], Ritika Gupta[ab], Poonam Sagar[ab], Geetika Bajaj[ab], Binduma Yadav[a], Vikas Rishi[a*], Bhupesh Goyal[e*], Ajay Kumar Srivastava[cd*], Nitin Kumar Singhal[a*]

[a] National Agri-Food Biotechnology Institute (NABI), Sector-81, S.A.S. Nagar, Mohali, Punjab, India

[b] Department of Biotechnology, Panjab University, Sector 25, Chandigarh, 160014, India

[c] Medicinal & Process Chemistry Division, CSIR-Central Drug Research Institute, Lucknow, 226031, India

[d] Academy of Scientific and Innovative Research, Ghaziabad, 201002, India

[e] School of Chemistry and Biochemistry, Thapar Institute of Engineering and Technology, Patiala 147004, Punjab, India

***Email:** nitin@nabi.res.in, ajayk.srivastava@cdri.res.in, bhupesh@thapar.edu, vikasrishi@nabi.res.in

 # Priyanka Garg, Nitesh Priyadarshi, and Mayur D. Ambule contributed equally.

Table of contents

Supporting Experimental and Figure Description.

Synthesis of β-D-Galactose-azide-sugar

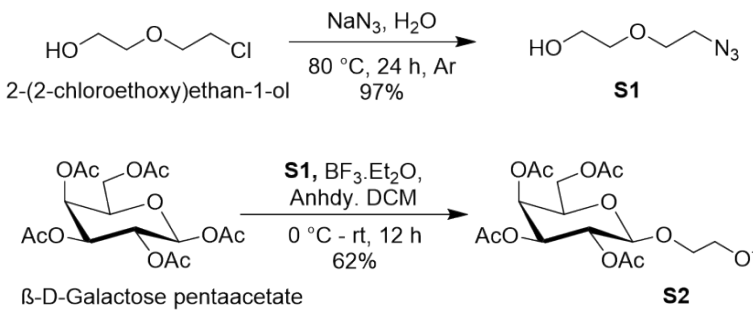

Synthesis of the clickable galactose tripod-amine

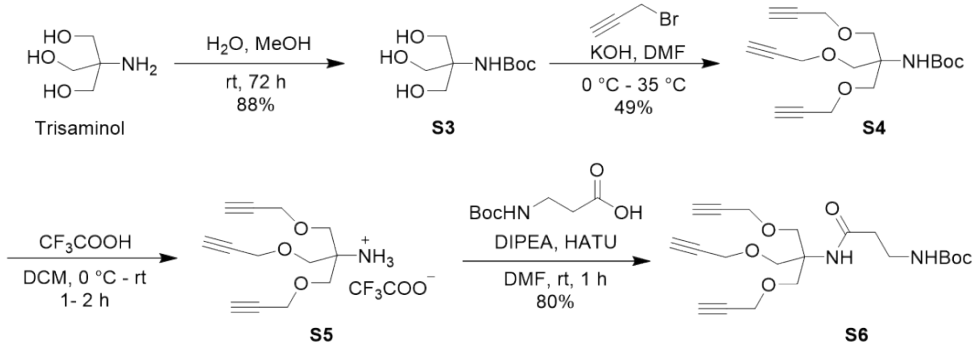

Synthesis of the galactose tripod

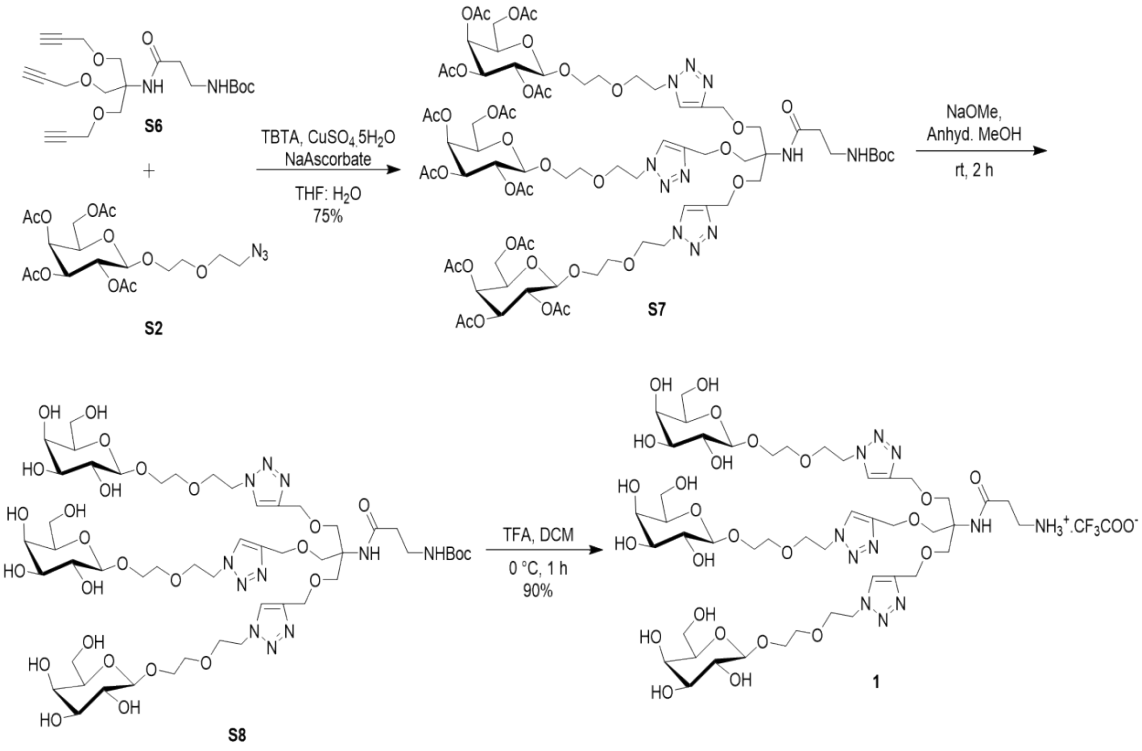

Figure S1. Schematic representation of synthesis of galactose tripod (Compound 1).

Compounds S1, S2, S3, S4, S5, S6 were synthesized according to previously reported method [1].

Compound (S7)

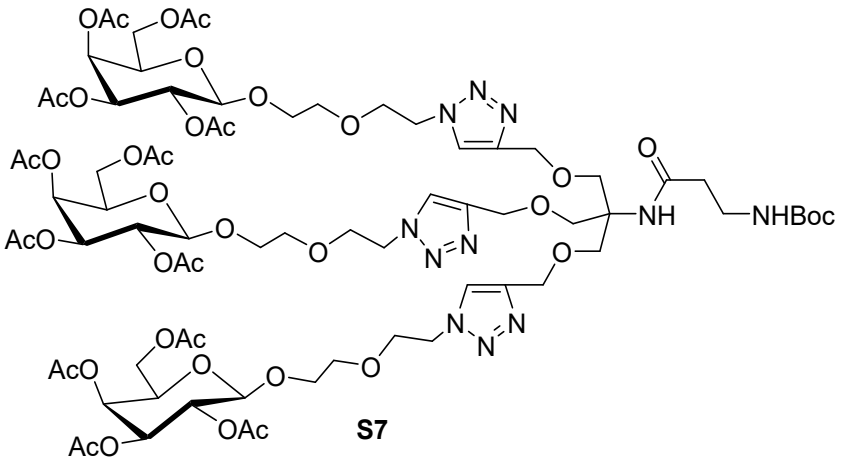

To a reaction vessel containing compound (**S6**) (250.0 mg, 0.615 mmol, 1.0 equiv), TBTA (65.2 mg, 61.50 µmol, 0.2 equiv), $CuSO_4.5H_2O$ (120.5 mg, 0.553 mmol, 0.9 equiv), sodium ascorbate (109.66 mg,0.553 mmol, 0.9 equiv), compound (**S2**) (1.02 g, 2.21 mmol, 3.6 equiv) were added and dissolved in a mixture of H_2O:THF 1:1 (15.0 mL), then the reaction was stirred at room temperature for 18 h. After completion of the reaction on the basis of TLC, ethyl acetate was added to the reaction mixture and washed with saturated aqueous NH_4Cl (2 × 20 mL), water (30 mL), and brine (30 mL). The separated organic layer was dried over Na_2SO_4, the solvent was removed under reduced pressure and the crude was purified by column chromatography (DCM: MeOH 9:1 to 8:2) affording pure compound **S5** as white solid (0.830 gm, 75%). **^{1}H NMR (400 MHz, $CDCl_3$)**: δ 7.67 (s, 3H), 6.32 (s, 1H), 5.43 (d, J = 3.7 Hz, 1H), 5.36 (d, J = 2.8 Hz, 3H), 5.16 (dd, J = 10.4, 8.0 Hz, 3H), 4.99 (dd, J = 10.5, 3.4 Hz, 3H), 4.58 (s, 6H), 4.50 (dd, J = 6.3, 4.2 Hz, 9H), 4.12 (qd, J = 11.2, 6.7 Hz, 6H), 3.92 (dt, J = 8.9, 5.6 Hz, 6H), 3.84 (t, J = 5.2 Hz, 6H), 3.77 (s, 6H), 3.71 – 3.64 (m, 3H), 3.60 (t, J = 4.6 Hz, 6H), 3.31 (t, J = 8.5 Hz, 2H), 2.32 (t, J = 6.0 Hz, 2H), 2.12 (s, 9H), 2.01 (d, J = 6.5 Hz, 18H), 1.96 (s, 9H), 1.38 (s, 9H). **^{13}C NMR (100 MHz, $CDCl_3$)**: δ 171.9, 170.5, 170.3, 170.2, 169.5, 156.1, 144.7, 123.7, 101.4, 70.9, 70.8, 70.3, 69.6, 69.1, 68.9, 67.1, 64.7, 61.3, 59.9, 50.3, 28.5, 20.8, 20.7, 20.6. HRMS (ESI) calculated for $C_{75}H_{111}N_{11}NaO_{39}$ $(M+Na)^+$: 1812.6938, found: 1812.6944. *m/z* MALDI-TOF MS calculated for $C_{75}H_{111}N_{11}NaO_{39}$ $(M+Na)^+$: 1812.6, found: 1812.6.

^{1}H NMR of S7

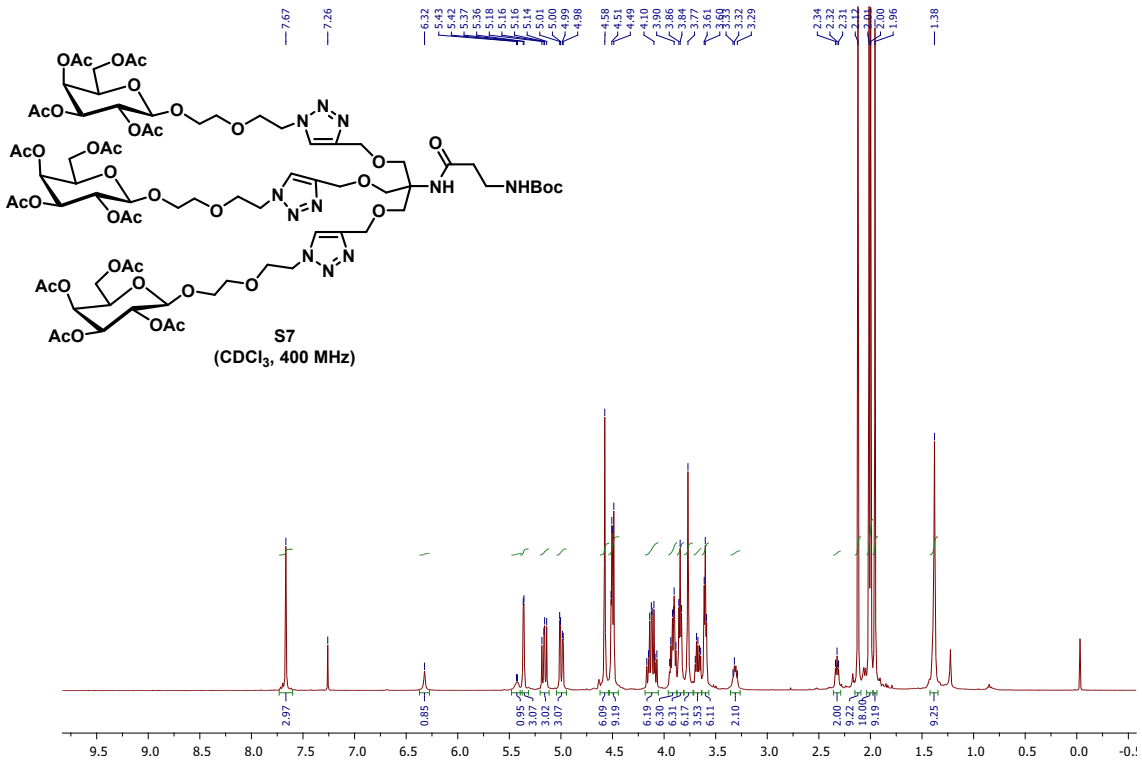

^{1}C NMR of S7

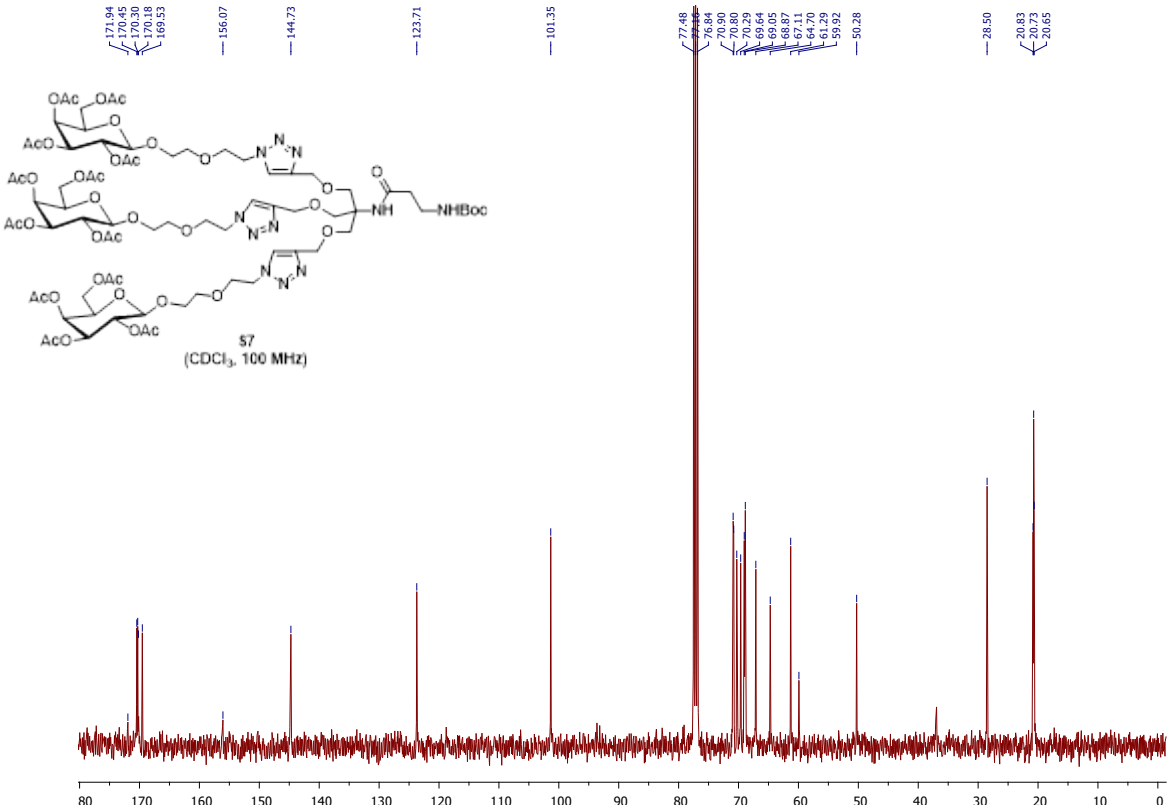

Figure S2. Method of synthesis of S7 and NMR of compound S7

MALDI-MS of S7

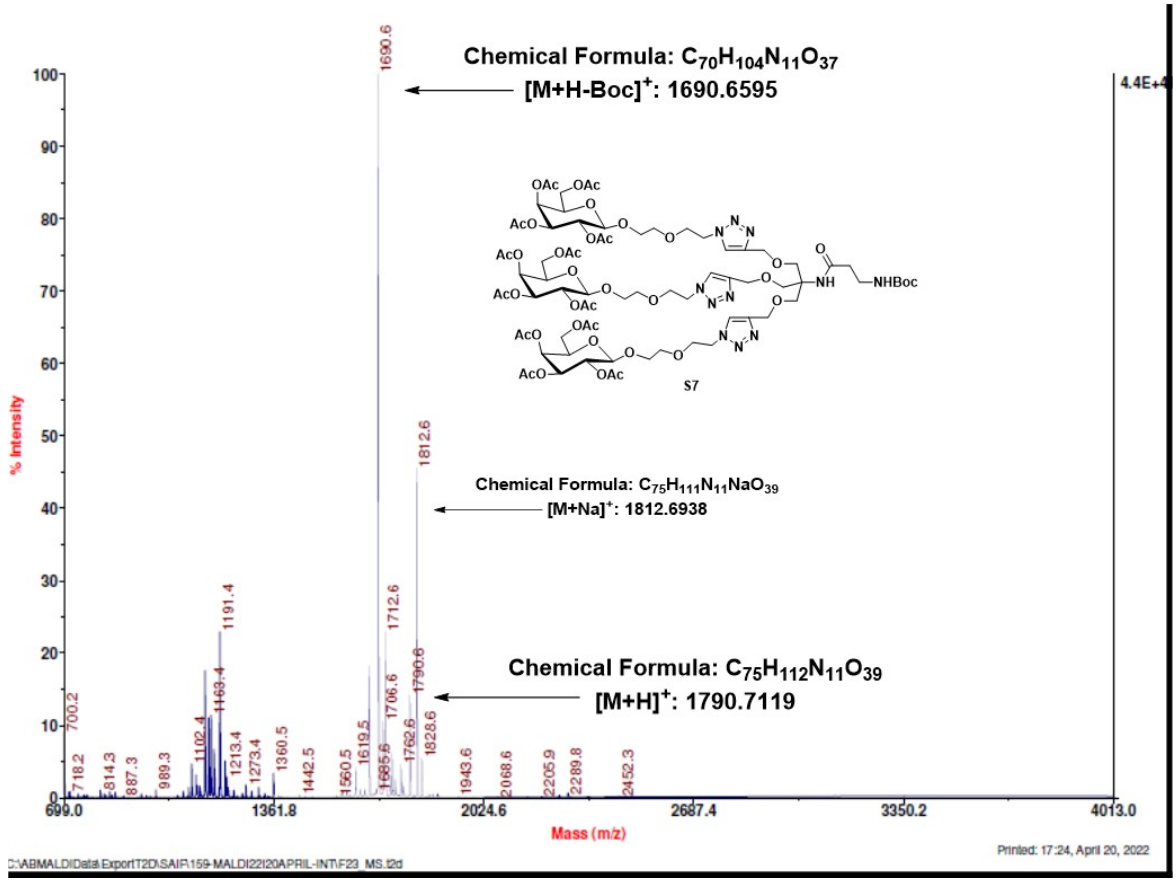

HRMS of S7

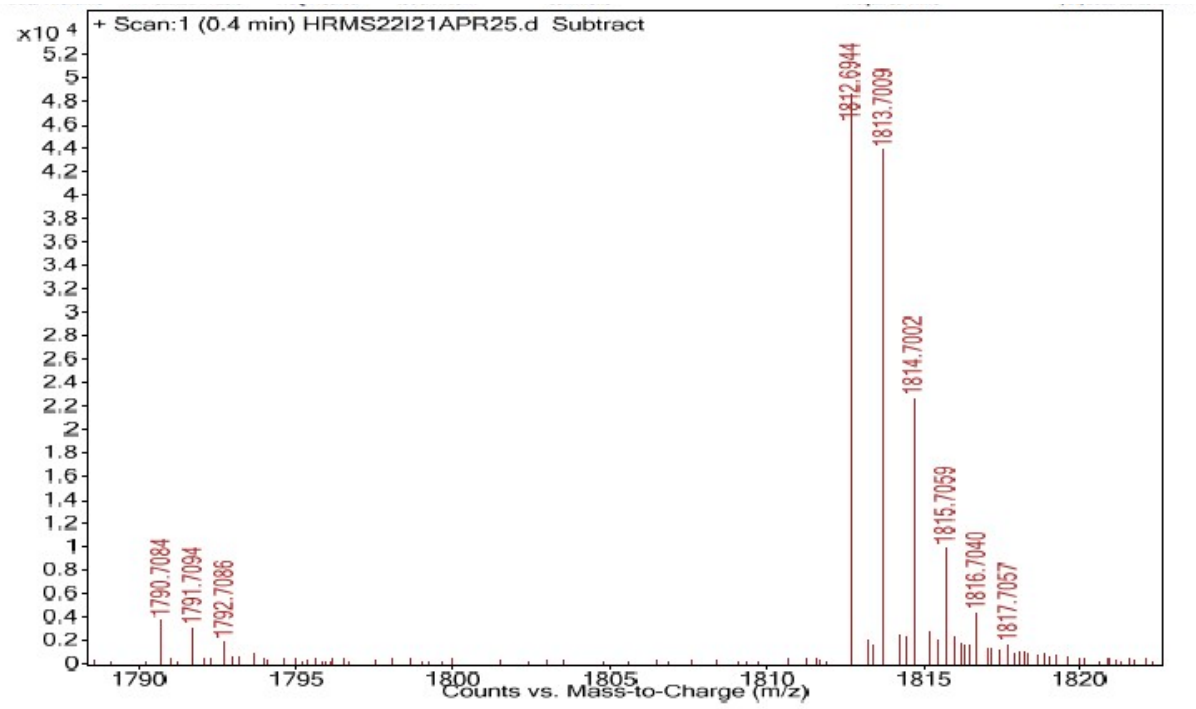

Figure S3. MALDI-MS and HRMS of compound S7.

Compound (S8)

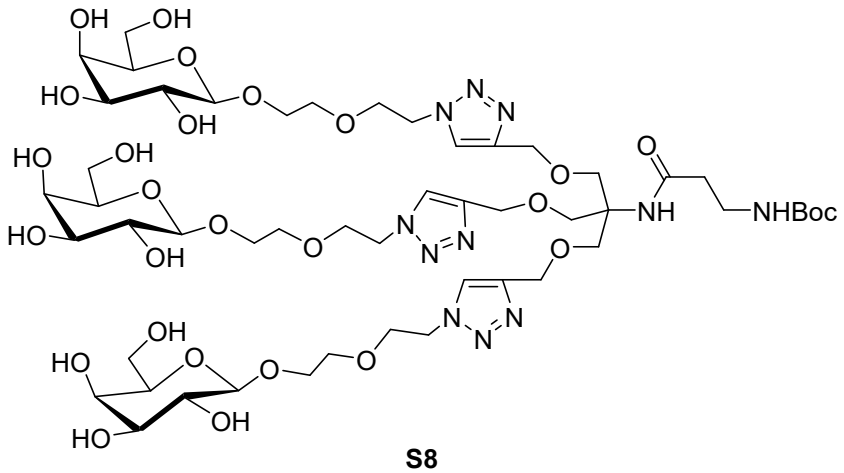

S8

A solution of compound **S3** (500.0 mg, 0.280 mmol, 1.0 equiv) in freshly distilled MeOH (20 mL) was treated with a solution of NaOMe (181.0 mg, 3.35 mmol, 12.0 equiv.). The reaction was stirred at room temperature under argon atmosphere. After 3-4 h the reaction was complete (based on TLC). The mixture was diluted with MeOH and neutralized by addition of Amberlite IR 120-H^+ resin, then the beads was filtered off and washed with MeOH. Finally the solvent was removed under reduced pressure and the crude was purified by using sephadex column G-20 affording compound **S8** as sticky oil (0.350 mg, 97%).**^{1}H NMR (400 MHz, CD_3OD)**: δ 8.06 (s, 3H), 4.63 – 4.55 (m, 12H), 4.26 (d, J = 7.4 Hz, 3H), 3.97 (dt, J = 8.8, 3.7 Hz, 3H), 3.91 (t, J = 5.0 Hz, 6H), 3.85 (d, J = 2.6 Hz, 3H), 3.74 (dd, J = 10.3, 5.8 Hz, 14H), 3.68 (dd, J = 10.5, 5.3 Hz, 8H), 3.55 – 3.49 (m, 8H), 3.25 (t, J = 5.9 Hz, 2H), 2.37 (t, J = 6.8 Hz, 2H), 1.40 (s, 9H). HRMS (ESI) calculated for $C_{51}H_{88}N_{11}O_{27}$ $(M+H)^+$: 1286.5851, found: 1286.5866. *m/z* MALDI-TOF MS calculated for C51H87N11NaO27 $(M+Na)^+$: 1308.5671, found: 1308.5.

^{1}H NMR of S8

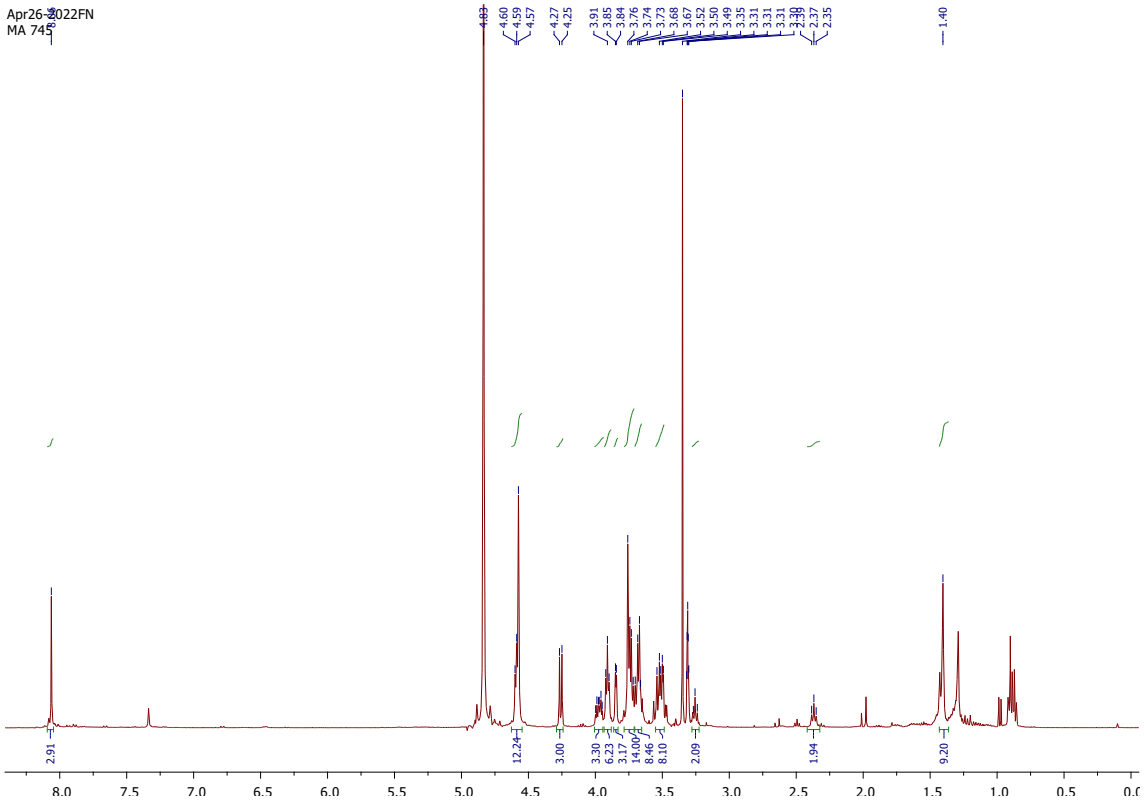

MALDI-MS of S8

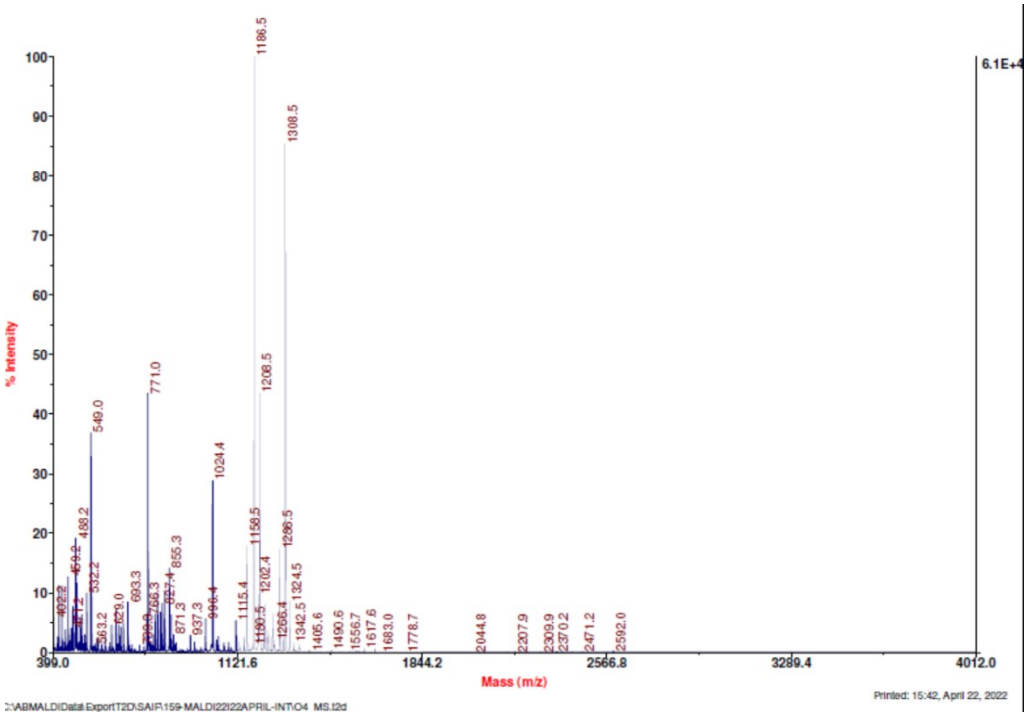

Figure S4. ^{1}H NMR and MALDI-MS of compound S8.

Compound 1

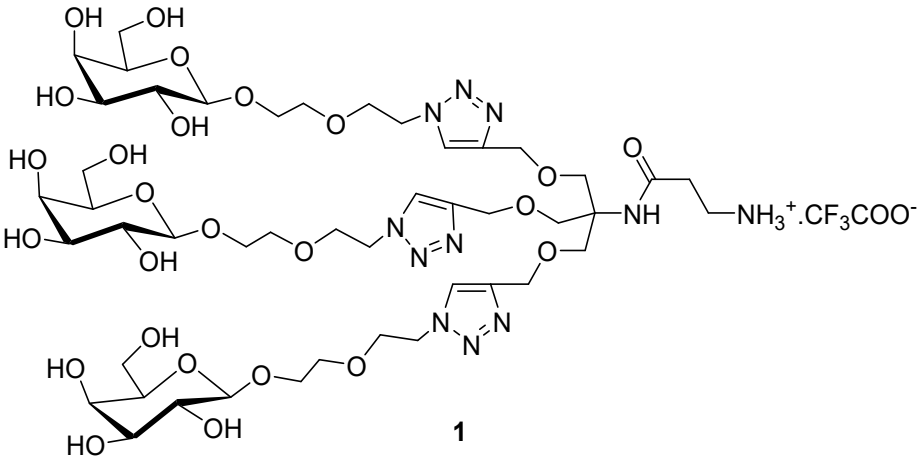

1

S10 (200 mg) was dissolved in 10.0 mL of DCM and TFA (5.0 mL) was added at 0 °C and stirred at rt. After completion of reaction, reaction mixture solvent was evaporated under reduced pressure to get compound **3** (yield 90%). Compound confirmed by HRMS and further used without purification. **HRMS (ESI)** calculated for $C_{46}H_{80}N_{11}O_{25}$ $(M+H)^+$: 1186.5327, found: 1186.5328. *m/z* MALDI-TOF MS calcd for $C_{46}H_{79}N_{11}NaO_{25}$ 1208.5146, $(M+Na)^+$: found 1208.5258.

^{1}H NMR of 1

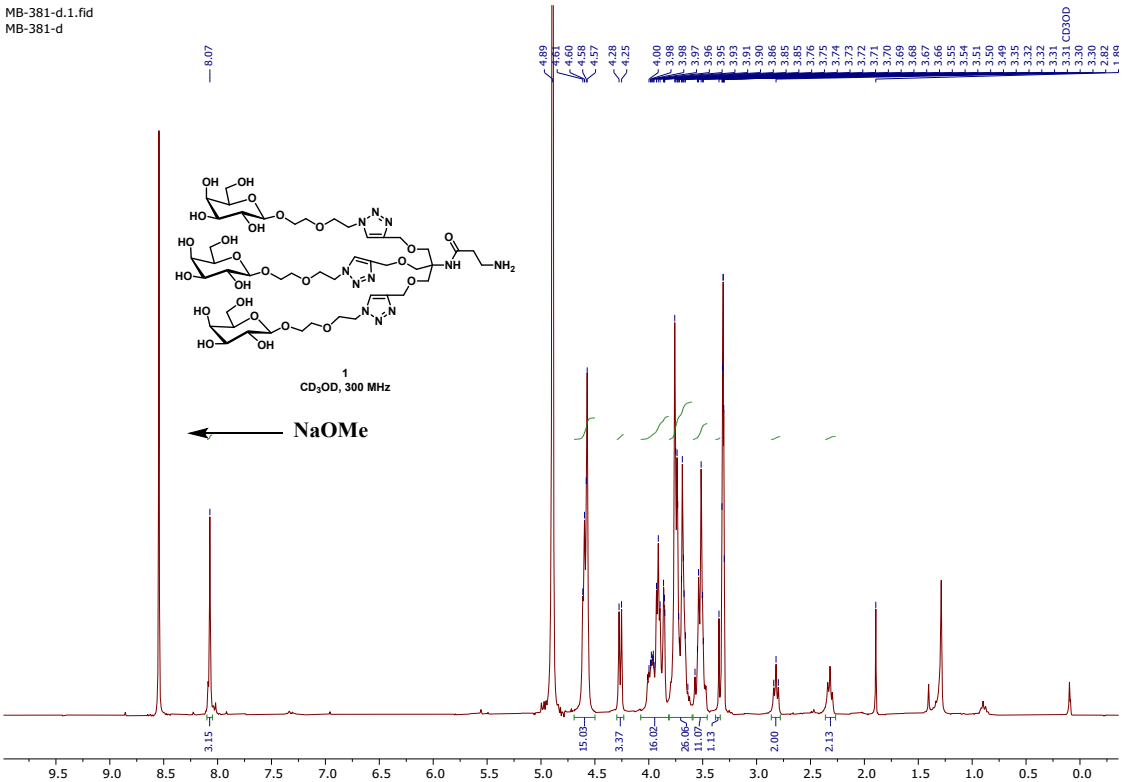

^{13}C NMR OF 1

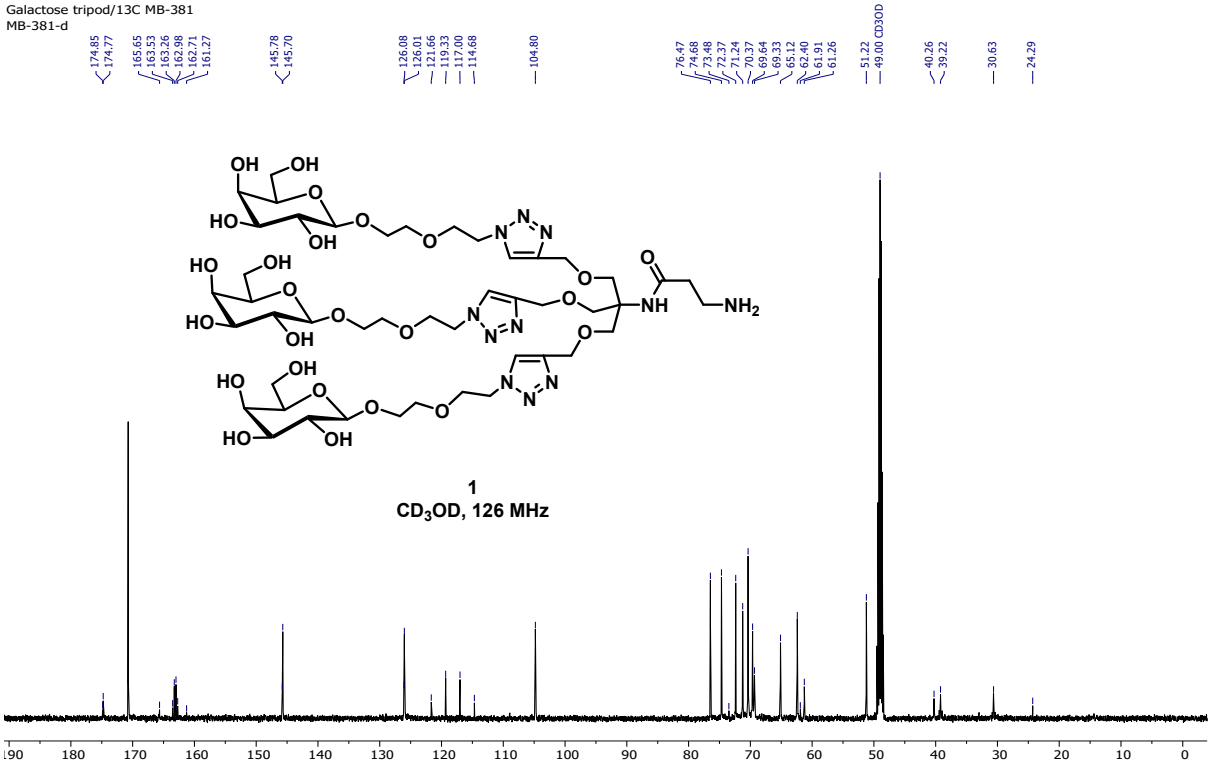

Figure S5. ^{1}H NMR and ^{1}C NMR of compound 1.

MALDI-MS of 1

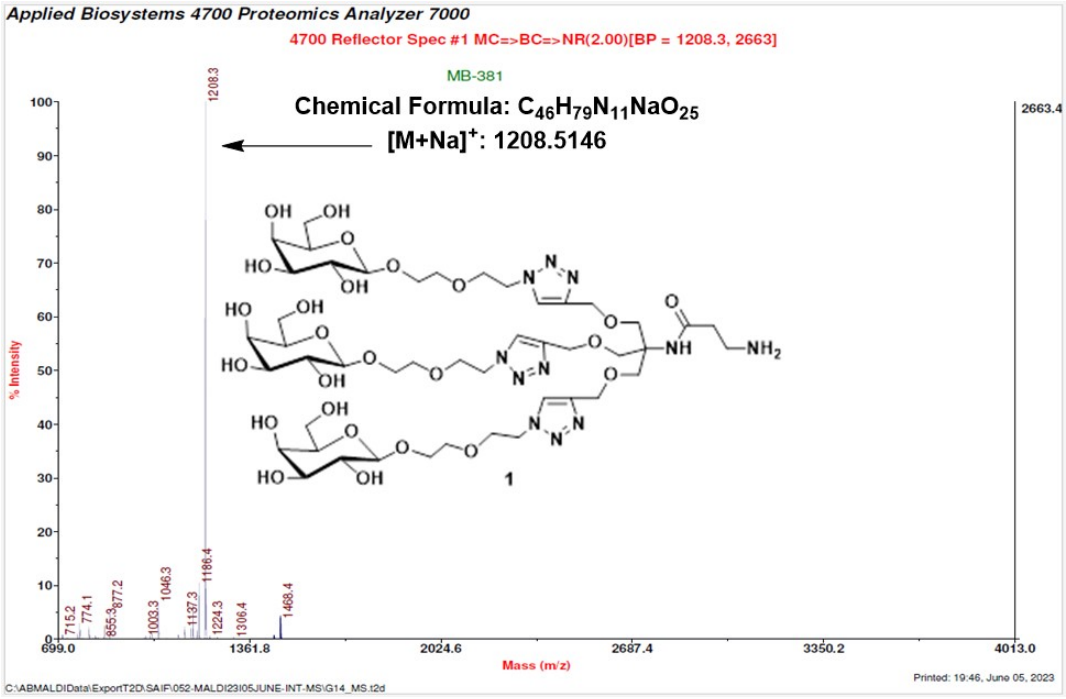

HRMS of compound 1.

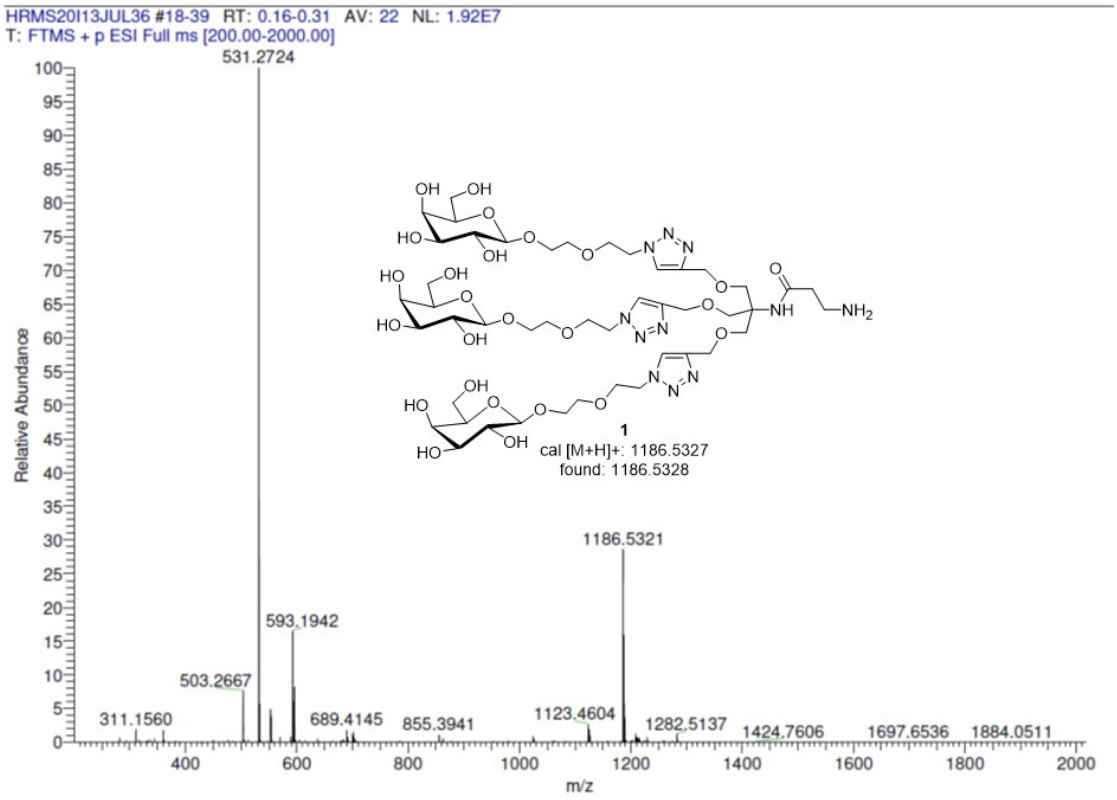

Figure S6. MALDI-MS and HRMS of compound 1.

LCMS of 1

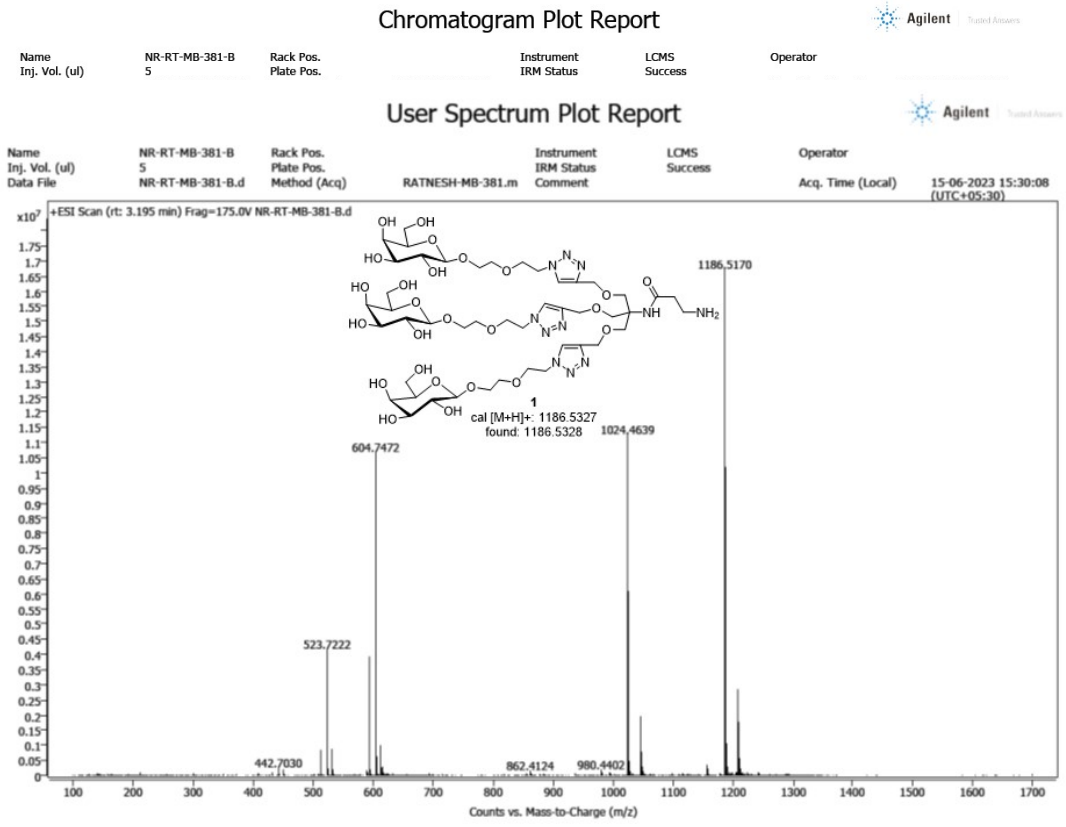

Figure S7. LCMS of compound 1.

Molecular docking and simulation studies

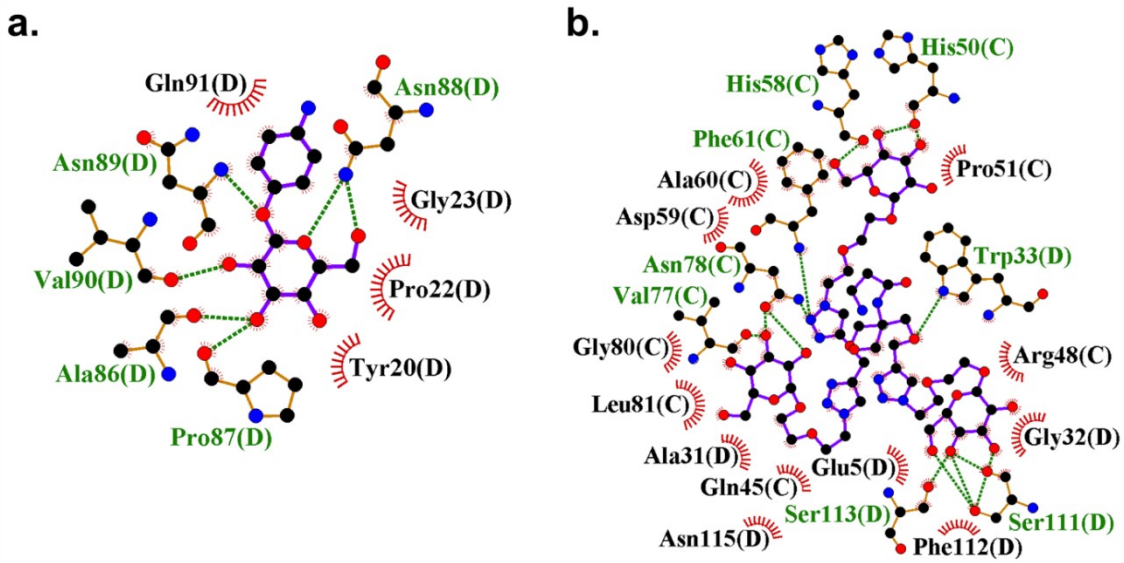

Figure S8. The 2D interaction maps displaying hydrophobic contacts of GM and GT with LecA are shown in panel a, and b respectively. Abbreviations: GM (Galactose monopod), GT (Galactose tripod).

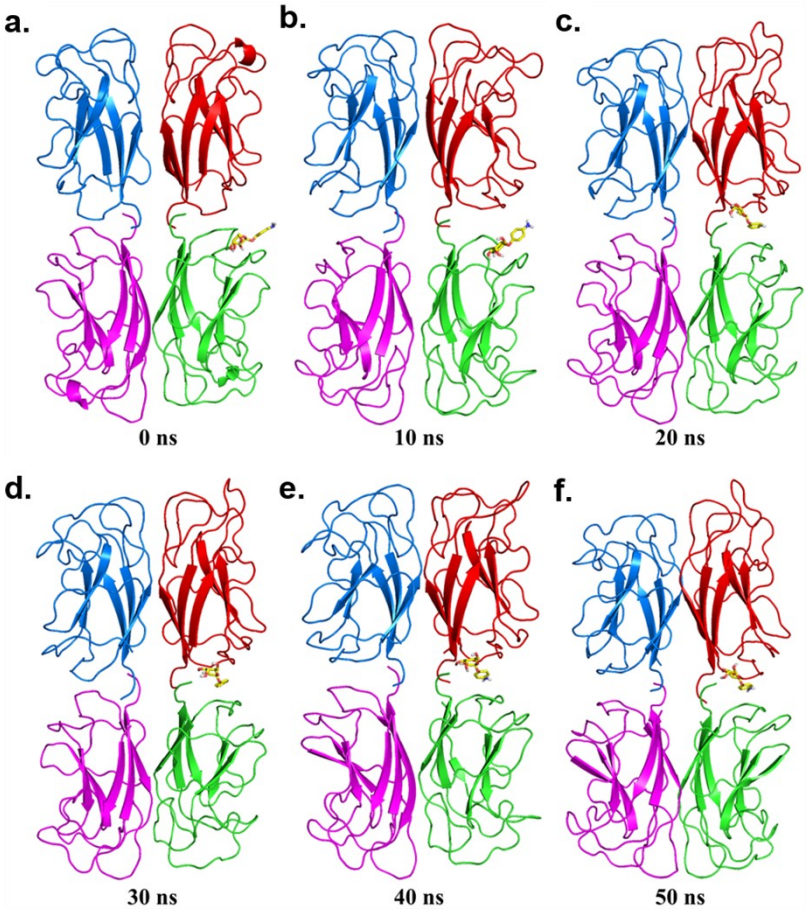

Figure S9. The conformational snapshots extracted from the MD trajectory of LecA–GM complex at various time intervals display the binding of GM to chains A and D of LecA. Abbreviations: GM (Galactose monopod), GT (Galactose tripod).

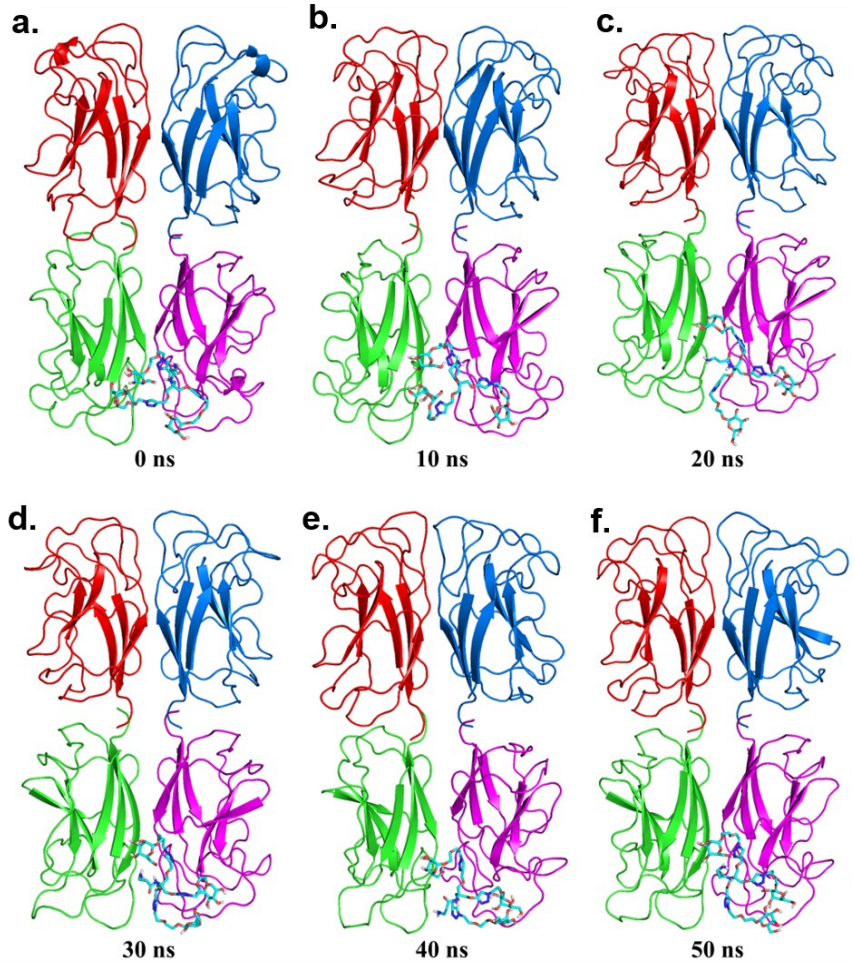

Figure S10. The conformational snapshots extracted from the MD trajectory of LecA–GT at various time intervals display the binding of GT in the central pocket and chains C, and D of LecA. Abbreviations: GM (Galactose monopod), GT (Galactose tripod).

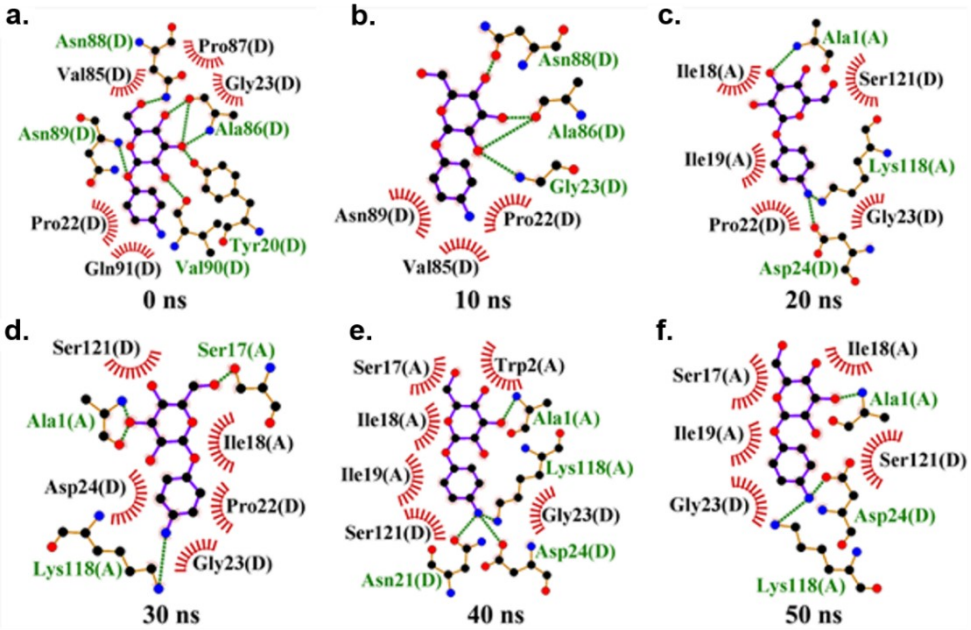

Figure S11. The 2D interaction map of conformational snapshots of LecA–GM complex display the hydrogen bond interactions and hydrophobic contacts of LecA residues with GM. Abbreviations: GM (Galactose monopod), GT (Galactose tripod).

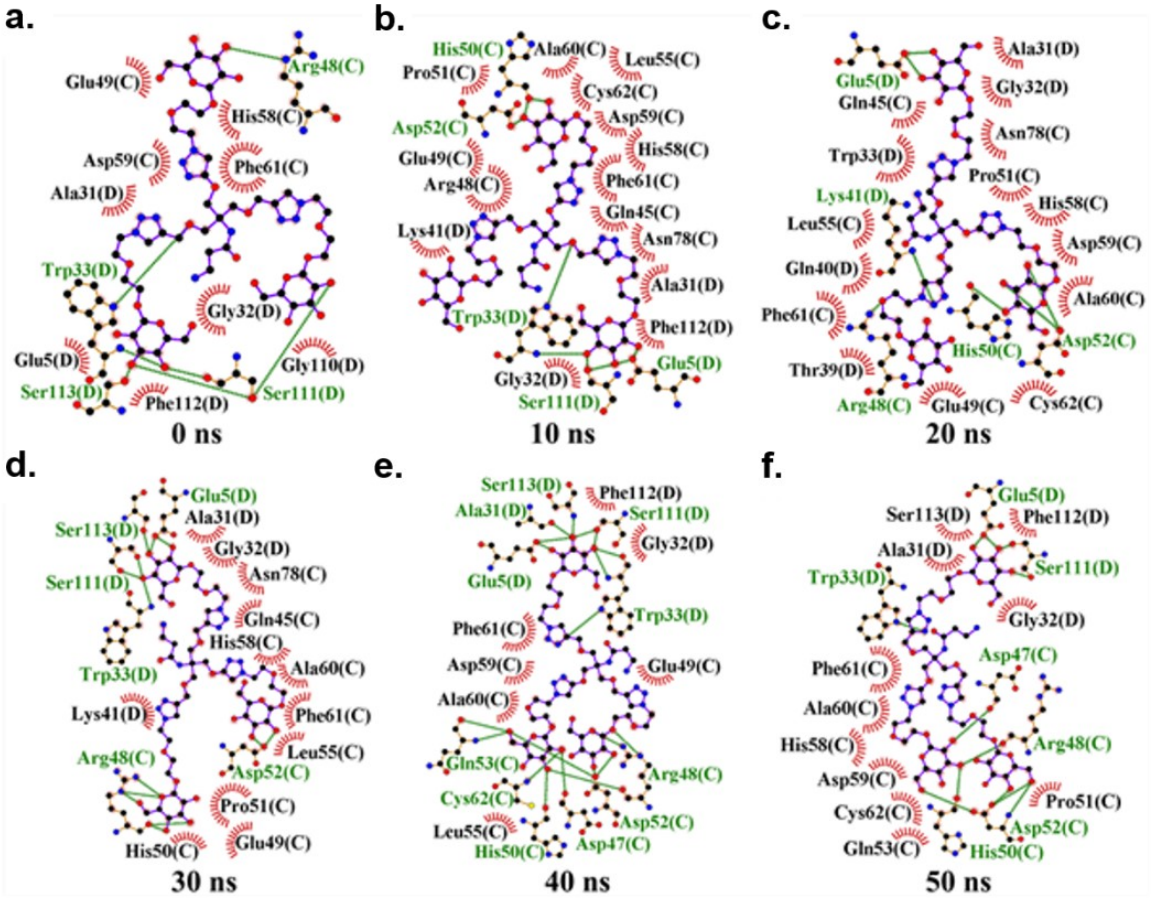

Figure S12. The 2D interaction map of conformational snapshots of LecA–GT complex display the hydrogen bond interactions and hydrophobic contacts of LecA residues with GT. Abbreviations: GM (Galactose monopod), GT (Galactose tripod).

Table S1. Molecular docking analysis of LecA–GM and LecA–GT complexes. The binding energies (kcal/mol) were evaluated using AutoDock.

Systems	AutoDock binding energy (kcal/mol)	LecA residues participating in intermolecular hydrogen bonds with GM and GT			LecA residues involved in hydrophobic contacts with GM and GT
		Residue	Atoms[a]	Distance (nm)	
LecA–GM	–5.9	Ala86 (D)	H:O	0.27	Tyr20 (D), Pro22 (D), Gly23 (D), Ala86 (D), Pro87 (D), Asn88 (D), Asn89 (D), Val90 (D), Gln91 (D)
		Pro87 (D)	H:O	0.20	
		Asn88 (D)	O:1Hδ2	0.23	
			O:1Hδ2	0.24	
		Asn89 (D)	O:HN	0.21	
		Val90 (D)	H:O	0.20	

LecA–GT	–6.6	His50 (C)	H:O	0.24	Gln45 (C), Arg48
		Asp52 (C)	O:HN	0.32	(C), His50 (C),
		His58 (C)	H:O	0.35	Pro51 (C), His58
		Phe61 (C)	N:HN	0.23	(C), Asp59 (C),
		Val77 (C)	H:O	0.35	Ala60 (C), Phe61
		Asn78 (C)	H:Oδ1	0.20	(C), Val77 (C),
			H:Oδ1	0.26	Asn78 (C), Gly80
			N:1Hδ2	0.30	(C), Leu81 (C),
		Trp33 (D)	O:1Hξ1	0.23	Glu5 (D), Ala31
		Ser111 (D)	O:HN	0.30	(D), Gly32 (D),
			H:Oγ	0.34	Trp33 (D), Ser111
			O:Hγ	0.26	(D), Phe112 (D),
		Ser113 (D)	H:Oγ	0.21	Ser113 (D),
					Asn115 (D)

[a]The atoms on the left side correspond to ligands and those on the right side correspond to LecA residues. Abbreviations: GM (Galactose monopod), GT (Galactose tripod).

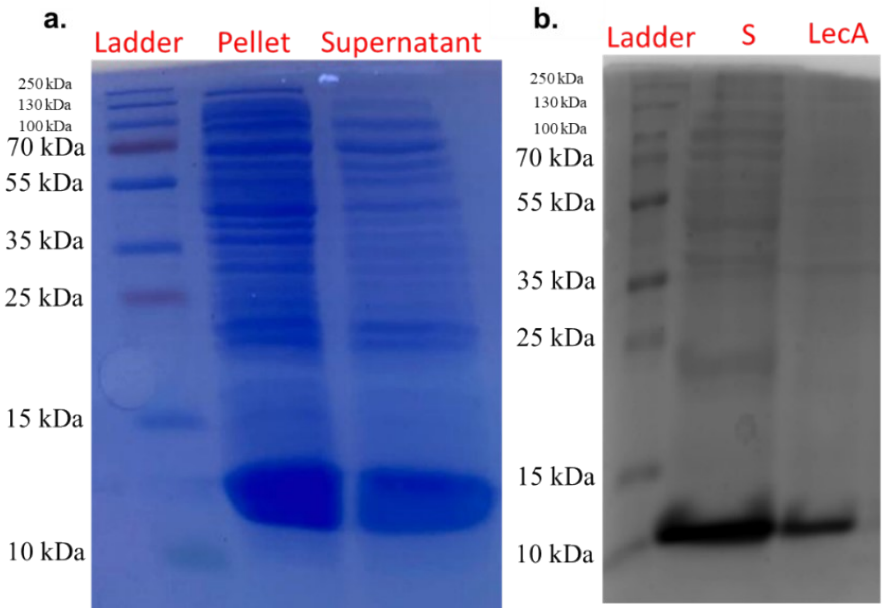

Figure S13. SDS gel electrophoresis showing a. LecA before purification, b. LecA after purification.

Abbreviations: S=supernatant.

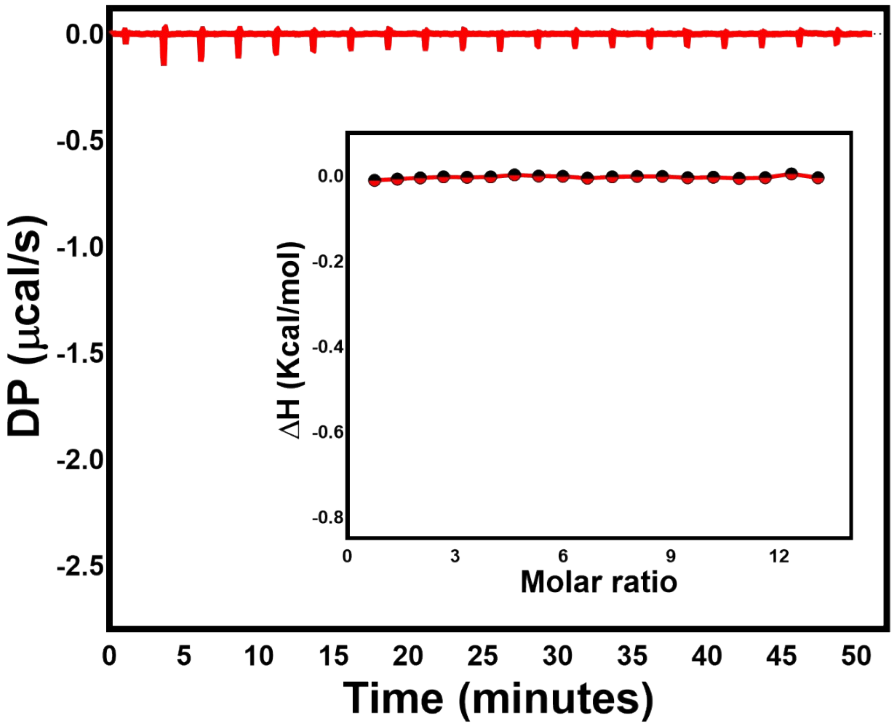

Figure S14. ITC graphs of GT titrations with Con A. The obtained raw data of ITC were plotted and fitted in the graph pad prism software. Abbreviations: GT (Galactose tripod), ConA (Concanavalin A).

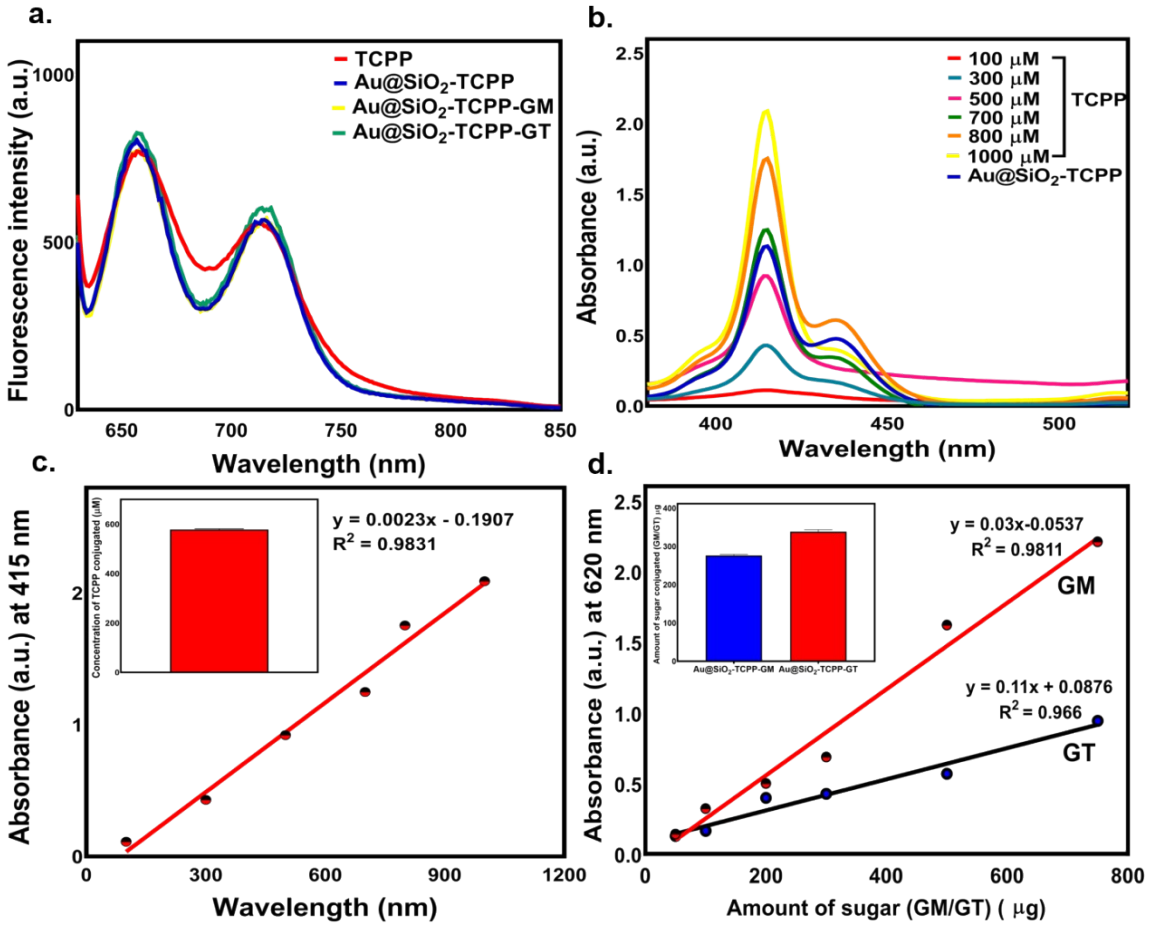

Figure S15. Characterization of glycan nanocomposites. a. Fluorescence spectra of TCPP, Au@SiO_2-TCPP, Au@SiO_2-TCPP-GM, Au@SiO_2-TCPP-GT. b. UV spectra of 100-1000 µM TCPP and Au@SiO_2-TCPP. c. Standard curve of TCPP (inset: bar graph showing the amount of TCPP conjugated in Au@SiO_2-TCPP). d. Anthrone test for estimating carbohydrate conjugated (inset: Bar graph showing the amount of sugar conjugated in nanocomposites. Abbreviations: GM (Galactose monopod), GT (Galactose tripod).

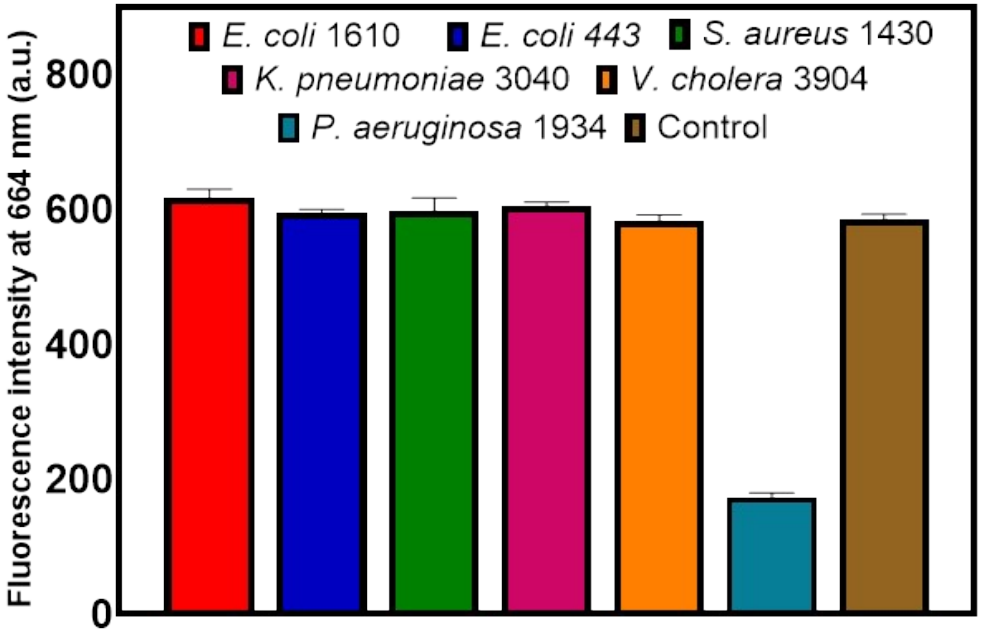

Figure S16: Fluorescence spectroscopic measurements at 664 nm with different bacteria (*E. coli* 1610, *E. coli* 443, *S. aureus* 1430, *K. pneumoniae* 3040, *V. cholera* 3904, *P. aeruginosa* 1934).

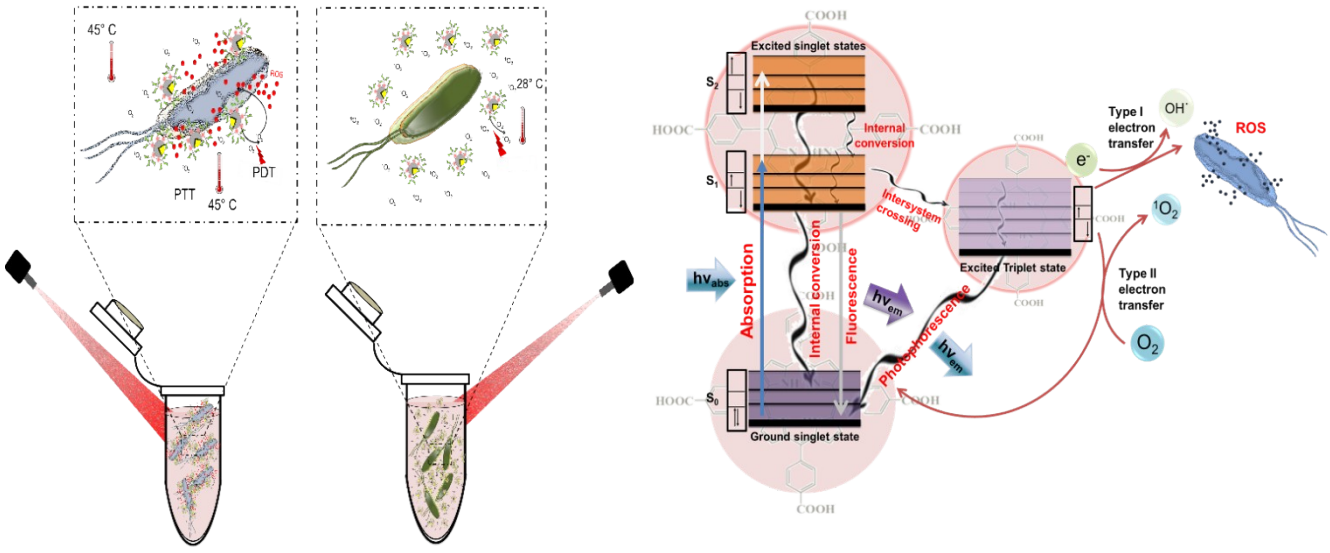

Figure S17. Schematic representation of Type II and photothermal mediated specific killing of *P. aeruginosa*.

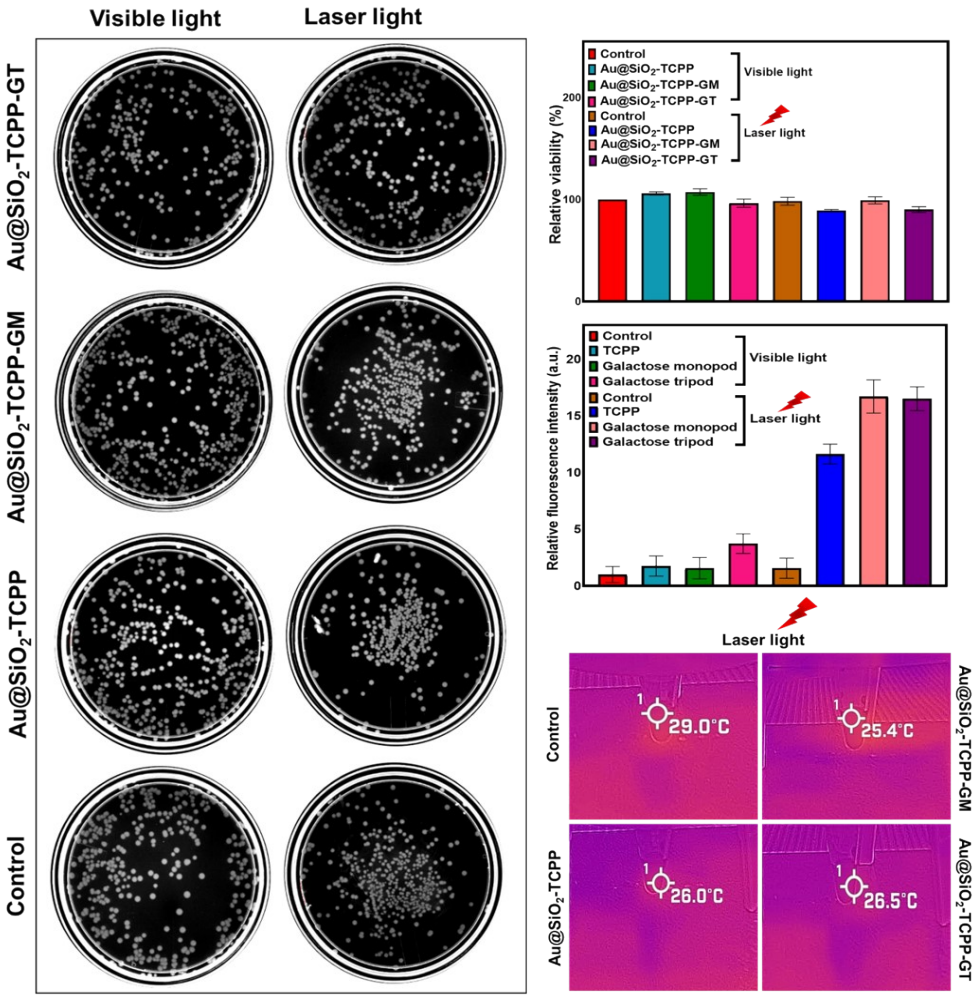

Figure S18. Synergistic photoablation of *E. coli.* a. Culture plate assay showing *E. coli* colonies, incubated with nanocomposites after visible and laser light irradiation. b. Percentage relative viability of *E. coli*, incubated with nanocomposites after visible and laser light irradiation. c. Measurement of ROS production by DCHF-DA assay. d. Photothermal therapy showing temperature change after laser light irradiation recorded using Flir1 pro photothermal camera. Abbreviations: GM (Galactose monopod), GT (Galactose tripod).

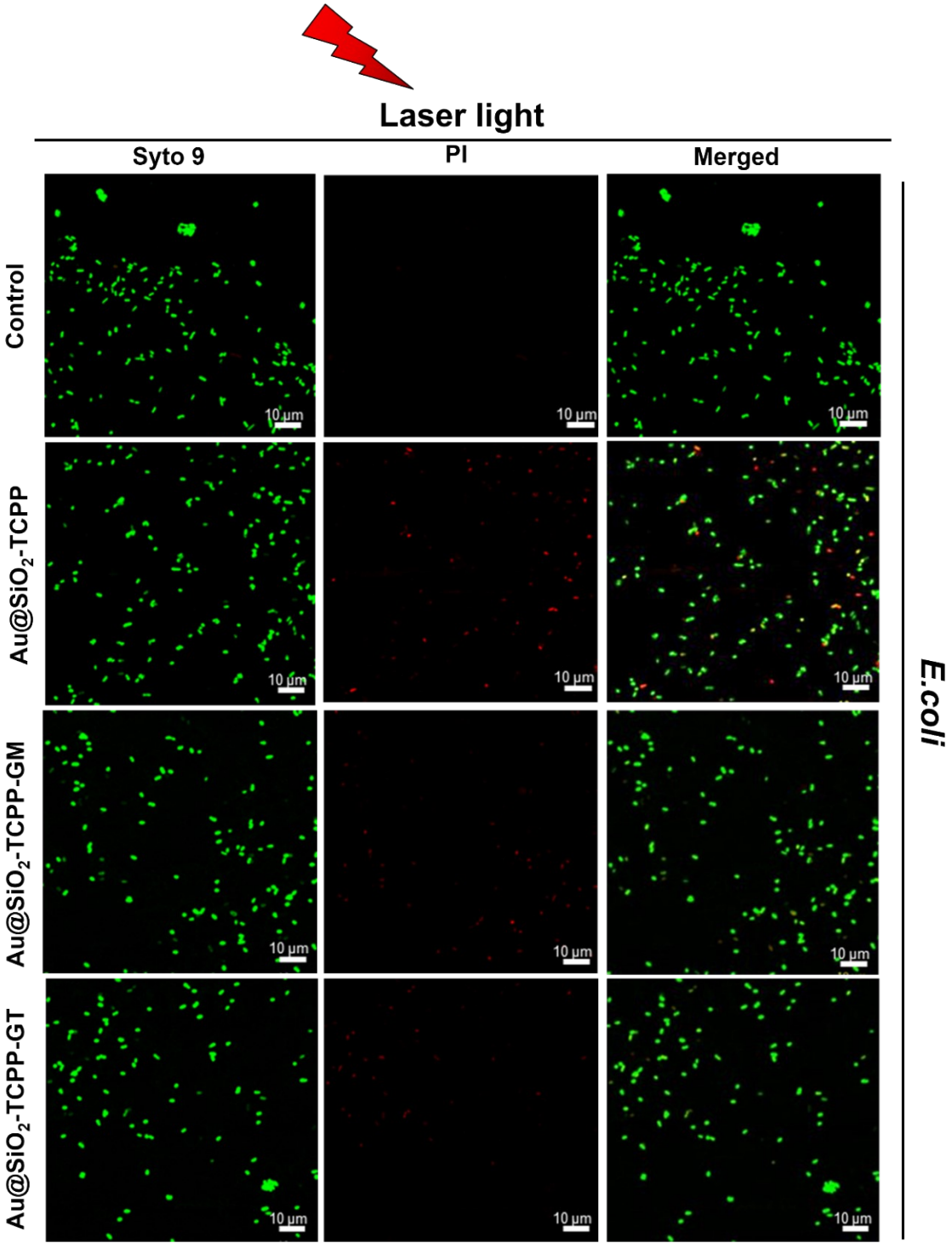
Laser light
Syto 9
PI
Merged
Control
Au@SiO2-TCPP
Au@SiO2-TCPP-GM
Au@SiO2-TCPP-GT
10 μm
E.coli

Figure S19. CLSM images of Live/dead (SYOT9 and PI) stained nanocomposite-treated *E. coli* after laser light irradiation. Scale bar: 10µm. Abbreviations: GM (Galactose monopod), GT (Galactose tripod).

Instruments utilized for carbohydrate characterization. NMR Spectroscopy at RT ^{1}H, and ^{13}C NMR spectra were obtained in $CDCl_3$, DMSO-d6, and CD_3OD as solvents (300 and 75 MHz/400 and 100 MHz). Chemical shifts of protons and carbon (δ) are reported in ppm, and coupling constants (J) are published in Hertz (Hz). The resonance multiplicity in ^{1}H NMR spectra is denoted by the letters s (singlet), d (doublet), t (triplet), and m (multiplet), with br denoting broad. In the ^{1}H- and ^{13}C-NMR spectra, residual protic solvents of $CDCl_3$ (^{1}H, 7.27 ppm; ^{13}C, 77.16 ppm and relative to tetramethylsilane (TMS) at = 0), CD_3OD (^{1}H, 3.31 ppm; ^{13}C, 49.0 ppm), and DMSO-d6 (^{1}H, 2.50 ppm; ^{13}C, 39.5 ppm) were employed as internal references. At the SAIF department of the CSIR-CDRI in Lucknow, India, high-resolution mass spectra (HRMS) were collected using a Q-TOF mass spectrometer. MALDI TOF MS were collected using a Micromass Tof Spec 2E Mass Spectrometer. Merck 60-120 and 100-200 mesh silica gels were used for column chromatography, and size-exclusion chromatography was used for size-exclusion chromatography (Sephadex G-20; in 100% MeOH). For purification in column chromatography, all solvents were distilled prior to use.

References

(1) N. Priyadarshi, M. D. Ambule, S. Kaushal, A. Kumar, P. Sagar, A. K. Srivastava and N. K. Singhal, Biosens Bioelectron, 2022, 201, 113969.